Gravity inversion of 2.5D faulted beds using depth-dependent density

V. Chakravarthi

National Geophysical Research Institute, Uppal Road, Hyderabad 500 007, India

A gravity inversion using Marquardt algorithm to simultaneously estimate four parameters of a 2.5D faulted bed in addition to regional gravity background is presented. The density contrast along the structure varied continuously with depth based on a parabolic function. Analysis of gravity anomalies over a synthetic fault structure using the present inversion unravelled the fact that the estimated parameters of a fault structure were independent of its strike length, as long as the profile bisected the fault plane. In case the profile failed to bisect the strike length, then the offset of the profile from the origin of the fault plane must be considered for reliable interpretation. A simulated parabolic density function of the Chintalpudi subbasin in India, was used to interpret the gravity anomalies of the Aswaraopet master fault. The estimated structure yielded a geologically plausible model that is consistent with borehole information.

Keywords: Fault structure, inversion, parabolic density function, strike length.

GRAVITY anomalies with a step-like appearance are often attributed to fault structures[1]. Interpretation of gravity anomalies due to such structures is then tantamount to solving four parameters, namely the depths to the top and bottom of the fault structure, angle of the fault plane and also locating its origin. Even though forward modelling schemes to compute gravity anomalies due to 2D objects with constant density are available[2], the practical utility of such schemes is limited because (1) the density of sedimentary rocks varies with depth[3–10] and (2) the parameters of a source body are not known in advance.

Because the strike lengths of many fault structures are often finite (2.5D) in nature[3] and also due to the fact that the density contrast varies with depth, 2.5D inversion schemes that use variable density models to simultaneously estimate both the parameters of the anomalous mass as well as regional background are often preferable than 2D strategies[11,12] to analyse the observed gravity anomalies.

In this communication, two mathematical strategies have been developed, namely a forward modelling to compute the gravity anomalies of a fault structure having finite strike length using the parabolic density function (PDF)[10,13], followed by an inversion to simultaneously estimate its parameters as well as regional gravity background. The efficacy of the inversion has been demonstrated with both theoretical and field gravity anomalies.

Let the z-axis be positive downward, with the x-axis transverse to the strike of a 2.5D faulted bed (Figure 1). Let z_T and z_B be the depths to the top and bottom of the faulted bed, with i being the angle of the fault plane. Further, let the profile AB runs through the origin $O(0, 0)$, along the x-axis and bisects the strike length $2Y$ of the fault structure along the y-axis. The gravity anomaly $g_f(x_m)$ at any point, $P(x_m, 0)$ on the profile can be expressed as,

$$g_f(x_m, 0) = 2G \int_{z_T}^{z_B} \Delta\rho(v)\{T_1 + T_2\}\mathrm{d}v, \tag{1}$$

where $T_1 = \tan^{-1}\dfrac{Y}{v}$, and

$$T_2 = \tan^{-1}\frac{Y(x_m + (v - z_T)\cot i)}{v\sqrt{(x_m + (v - z_T)\cot i)^2 + v^2 + Y^2}}.$$

Here G is the universal gravitational constant and $\Delta\rho(v)$ is the density contrast at any depth $z = v$, as represented by the parabolic density function[10,13]

$$\Delta\rho(v) = \frac{\Delta\rho_0^3}{(\Delta\rho_0 - \alpha v)^2}. \tag{2}$$

Here $\Delta\rho_0$ is the density contrast extrapolated to the ground surface and α is a constant which can be obtained by fitting eq. (2) to the known subsurface geological information[10,13].

It is to be noted that eq. (1) is strictly valid for the profile AB, which runs across and bisects the strike length $2Y$ of the fault plane (Figure 1). In case the profile runs at an offset s from the origin of the fault plane along the y-axis (shown as $A'B'$ in Figure 1), then the anomalous field along the profile can be calculated by substituting $Y + s$ and $Y - s$ for Y in eq. (1), and taking the average. The

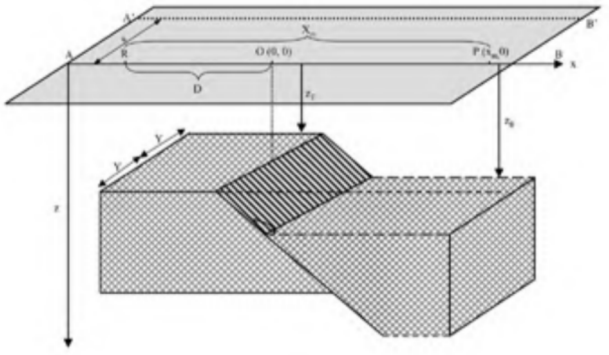

Figure 1. Geometry of a 2.5D faulted bed.

e-mail: vcvarthi@rediffmail.com

effect of offset s is illustrated with two gravity profiles EE' and FF' that are generated at $s = 0$ km and $s = 40$ km over a 2.5D faulted bed (Figure 2). It can be seen from Figure 2 that the magnitude of the gravity anomaly over a fault structure is dependent on the offset of the profile, and the fact that the present inversion is also dependent on the magnitude of the anomalous field necessitates considering the offset as a significant parameter in the interpretation for reliable results.

In case of a concealed fault, the origin of the fault plane $O(0, 0)$, also becomes an unknown parameter. If D is the distance of the origin $O(0, 0)$ from an arbitrary reference point R on the profile (Figure 1) and X_m is the distance of the point of observation $P(x_m, 0)$ from R, then by substituting $\hat{x}_m$ (where $\hat{x}_m = X_m - D$) for x_m in eq. (1) is tantamount to calculating the gravity anomaly with respect to R. Here, the measurement interval of observation is considered with respect to a reference point R on the profile.

Further, the gravity anomaly of a faulted bed can seldom be isolated perfectly from the interference of neighbouring sources and sometimes such interference can be described with a second order polynomial[14]. In the presence of regional gravity background, eq. (1) takes the form

$$g_f(\hat{x}_m, 0) = 2G\Delta\rho_0^3 \int_{z_T}^{z_B} \frac{1}{(\Delta\rho_0 - \alpha v)^2}\{T_1 + T_2\}\mathrm{d}v + \sum_{n=0}^{2} a_n \hat{x}_m^n, \tag{3}$$

where a_n, $n = 0, 1, 2$ are coefficients of the polynomial.

Inversion of gravity anomalies is an optimization procedure to estimate four shape parameters, namely z_T, z_B, D and i of a 2.5D faulted bed in addition to three coefficients of the polynomial, by fitting eq. (3) to the observed gravity anomalies in least squares approach using Marquardt algorithm[15]. The application of Marquardt algorithm was described by Murthy[1] and Chakravarthi[13]. In this case the system of normal equations is given by

$$\sum_{m=1}^{N_{obs}} \sum_{j=1}^{7} \frac{\partial g_f(\hat{x}_m)}{\partial a_{j'}} \frac{\partial g_f(\hat{x}_m)}{\partial a_j}(1 + \delta_{jj'}\lambda)\mathrm{d}a_j$$

$$= \sum_{m=1}^{N_{obs}} [g_{obs}(\hat{x}_m) - g_f(\hat{x}_m)] \frac{\partial g_f(\hat{x}_m)}{\partial a_{j'}}, \quad j' = 1, \ldots, 7, \tag{4}$$

where $\mathrm{d}a_j$, $j = 1, 2, \ldots, 7$ are improvements to the four parameters of the fault structure and three coefficients of the regional anomaly respectively. Here λ is the damping factor. The partial derivatives in eq. (4) are calculated by a numerical approach. The seven improvements solved using eq. (4) are added to or subtracted from the existing parameters until (i) the specified number of iterations is completed, or (ii) the misfit[14] falls below a predefined

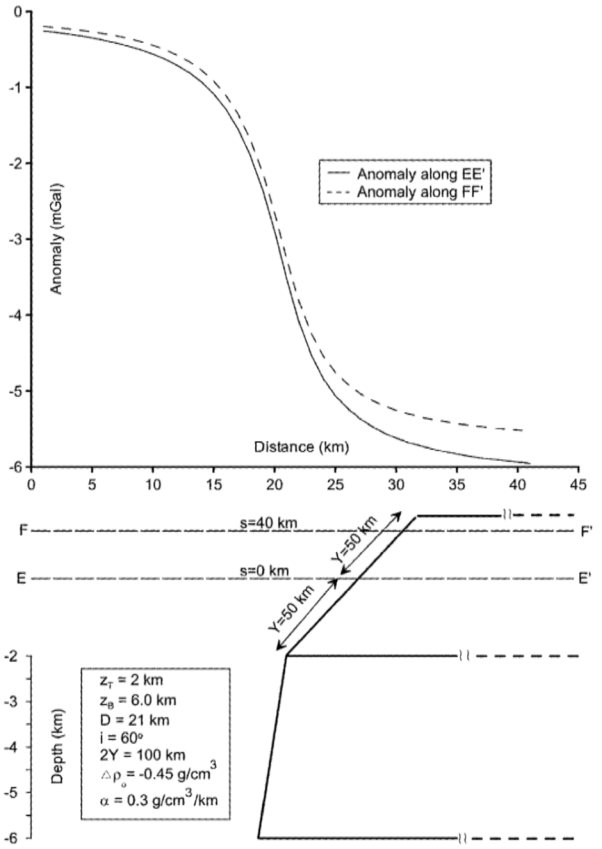

Figure 2. Gravity anomalies along two profiles, one passing through the origin (EE') and the other running at an offset $s = 40$ km, (FF') of a theoretical fault model.

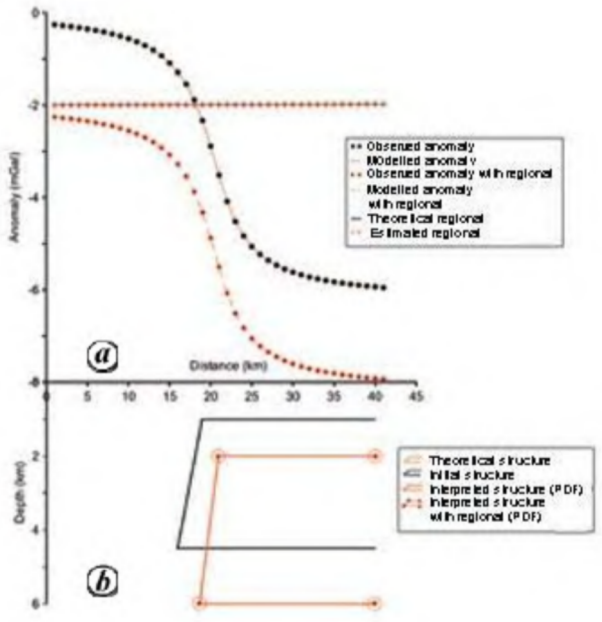

Figure 3. Interpretation of gravity profile EE' both with and without regional background.

Table 1. Analysis of gravity profile *EE′* both with and without regional background for different initial models. Interpreted parameters of field gravity data are also shown

Model	Structure	Initial parameter				Interpreted parameter				Misfit function	
		z_1 (km)	z_2 (km)	D (km)	i (degree)	z_1 (km)	z_2 (km)	D (km)	i (degree)	Initial	Final
I*	$2^{1/2}$D	1.0	4.5	19.0	40	2.0	6.0	21.0	60	341.0	0.0
	2D	1.0	4.5	19.0	40	2.0	6.0	21.0	60	373.0	0.0
II	$2^{1/2}$D	0.2	3.0	15.0	30	2.0	6.0	21.0	60	2902.0	0.0
	2D	0.2	3.0	15.0	30	2.0	6.0	21.0	60	2982.0	0.0
With regional background											
I*	$2^{1/2}$D	1.0	4.5	19.0	40	2.0 (–2.0)	6.0 (4E-4)	21.0 (1E-6)	60	117.0	0.0
	2D	1.0	4.5	19.0	40	2.0 (–1.9)	6.0 (17E-4)	21.0 (1E-6)	60	124.7	0.0
II	$2^{1/2}$D	0.2	3.0	15.0	30	2.0 (–2.0)	6.0 (4E-4)	21.0 (1E-6)	60	1889.0	0.0
	2D	0.2	3.0	15.0	30	2.0 (–1.9)	6.0 (17E-4)	21.0 (1E-6)	60	1947.0	0.0
Field example											
I+	$2^{1/2}$D	0.05	1.5	20.0	70	0.23 (0.36)	3.0 (–0.09)	19.8 (2E-3)	148	250.2	0.9
	2D	0.05	1.5	20.0	70	0.22 (0.71)	2.8 (–0.08)	19.8 (2E-3)	150	204.5	0.8
II	$2^{1/2}$D	0.2	2.2	19.5	90	0.24 (0.36)	3.0 (–0.09)	19.8 (2E-3)	148	154	0.9
	2D	0.2	2.2	19.5	90	0.21 (0.71)	2.8 (–0.08)	19.7 (2E-3)	150	118	0.7

*Shown graphically in Figure 3. +Shown graphically in Figure 5.

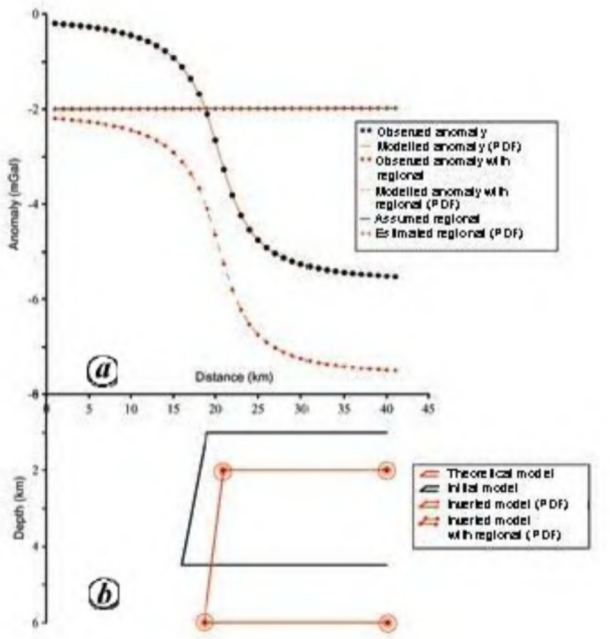

Figure 4. Interpretation of gravity profile *FF′* both with and without regional background.

allowable error, or (iii) the damping factor attains an unusually large value.

Figure 3 shows the interpretation of the gravity profile *EE′*. To invert the anomaly (Figure 3 *a*), $\Delta\rho_0$ and α are derived based on the known density–depth information, while the half strike length Y of the fault structure is obtained from Figure 2. The initial model with assumed parameters (model I of Table 1) is shown in Figure 3 *b*. The inversion performed 24 iterations before it got terminated. The misfit reduced drastically from 341.3 to 2.14 at the end of the third iteration and then gradually reached zero at the end of the 24th iteration. The estimated parameters subsequent to inversion are given in Table 1 and graphically shown in Figure 3 *b*.

Further, to study the effect of strike length on the interpretation, the same gravity profile *EE′* was also inverted using the 2D algorithm of Chakravarthi and Sundararajan[14]. The estimated parameters subsequent to inversion are also given in Table 1. It is interesting to note from Table 1 that the estimated parameters based on 2D inversion coincide exactly with those estimated from 2.5D inversion, implying that the strike length does not affect the inversion as long as the profile bisects the strike length. The anomaly shown in Figure 3 *a* was also interpreted using a different initial model (model II of Table 1) with both 2.5D and 2D algorithms. It was found that the estimated parameters remained the same.

Figure 4 *a* shows the interpretation of the gravity profile *FF′*, which runs across the strike of the fault plane at an offset $s = 40$ km from the origin $O(0, 0)$. The offset s of the profile is obtained from Figure 2. In this case, the initial model parameters are similar to those of model I of Table 1. The inversion took 25 iterations and the estimated parameters are given in Table 2 and shown in Figure 4 *b*. The effect of offset s was studied by letting $s = 0$ in the inversion (estimated parameters are given in Table 2). It was found that the parameters z_T, z_B and i subsequent to inversion were underestimated. Interpretation of the same profile using a different initial model (model II of Table 2) also substantiates the same.

In this context, to study the effect of regional background on the inversion, a polynomial, $a_0 + a_1x + a_2x^2$, with coefficients $a_0 = -2.0$, $a_1 = 4\text{E-}04$ and $a_2 = 1\text{E-}06$

Table 2. Analysis of gravity profile *FF'* both with and without regional background for different initial models

		Initial parameter				Interpreted parameter				Misfit function	
Model	Offset s (km)	z_1 (km)	z_2 (km)	D (km)	i (degree)	z_1 (km)	z_2 (km)	D (km)	i (degree)	Initial	Final
Without regional background											
I*	40.0	1.0	4.5	19.0	40	2.0	6.0	21.0	60	334.7	0.0
	0.0	1.0	4.5	19.0	40	1.9	5.4	21.0	54	407.5	0.0
II	40.0	0.2	3.0	15.0	30	2.0	6.0	21.0	60	2897.4	0.0
	0.0	0.2	3.0	15.0	30	1.9	5.4	21.0	54	3085.6	0.0
With regional background											
I*	40.0	1.0	4.5	19.0	40	2.0 (–2.0)	6.0 (4E-4)	21.0 (1E-6)	60	115.0	0.0
	0.0	1.0	4.5	19.0	40	1.9 (–1.97)	5.4 (4E-3)	21.0 (–4E-6)	54	143.0	0.0
II	40.0	0.2	3.0	15.0	30	2.0 (–2.0)	6.0 (4E-4)	21.0 (1E-6)	60	1886.4	0.0
	0.0	0.2	3.0	15.0	30	1.9 (–1.97)	5.4 (4E-3)	21.0 (–4E-6)	54	2031.4	0.0

*Shown graphically in Figure 4.

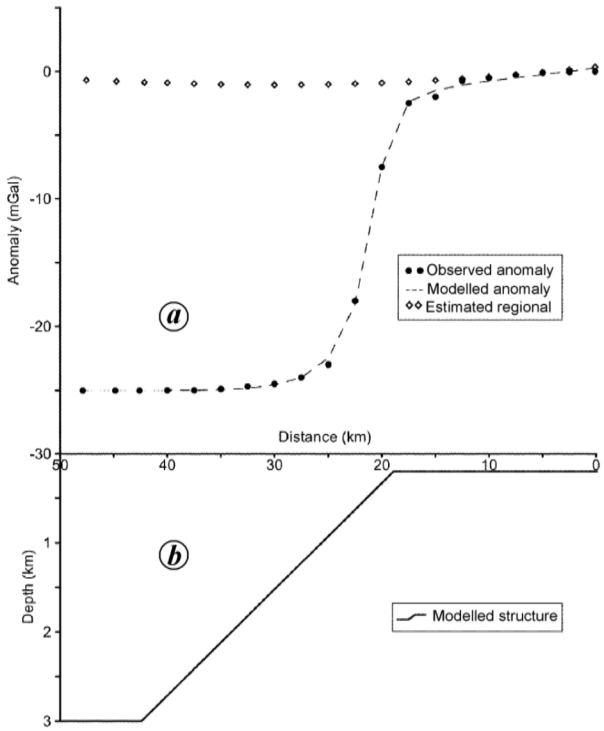

Figure 5. Analysis of gravity anomalies of Aswaraopet master fault, India.

was added to both the anomaly profiles shown in Figures 3 *a* and 4 *a*, and then inverted using the procedure outlined. The estimated parameters along with the coefficients of regional background subsequent to inversion are given in Tables 1 and 2. The interpreted structures are shown in Figures 3 *b* and 4 *b* respectively. The estimated regional in either case (Figures 3 *a* and 4 *a*) closely mimics the actual one. Further, the estimated parameters remain the same even in the presence of the regional background, implying that the inversion was insensitive to its effect. The inversion performed with different initial models also yielded similar results (Tables 1 and 2).

The Chintalpudi sub-basin represents the southeasterly continuation of the Kothagudem sub-basin of the Pranhita–Godavari valley. The Archaean gneisses form the basement for the Gondwana sequence within the sub-basin. On the eastern side, the basin is bounded by the well-known Aswaraopet master fault, which is exposed to the surface and strikes NNW–SSE over a length of 20 km. The Oil and Natural Gas Corporation Ltd (ONGC), India drilled a borehole in the basin[16] and encountered the basement at a depth of 2.935 km. Values of $\Delta\rho_0$ and α of the PDF (eq. 2) were –0.5 g/cm^3 and 0.1811 g/cm^3/km respectively[17]. For the present study, a gravity profile of 40 km length (Figure 5 *a*) bisecting the strike of the fault was considered for both 2D and 2.5D inversion. The initial model with parameters $z_T = 0.05$ km, $z_B = 1.5$ km and $i = 70°$ is shown in Figure 5 *b*. The estimated parameters are given in Table 1 and graphically shown in Figure 5 *b*. The computed regional background followed by inversion is also shown in Figure 5 *a*. The interpretation carried out using a different initial model (model II of Table 1) in either case yielded more or less the same results. The fact that the vertical throw of the fault (i.e. $z_B - z_T = 2.765$ km) estimated from the present inversion more or less coincides with the total thickness of the Gondwana sediments (2.935 km) in the basin, demonstrates the validity and applicability of the algorithm.

A gravity inversion using Marquardt algorithm to simultaneously estimate four parameters of a 2.5D faulted bed as well as regional gravity background is presented. The significance of strike length of the structure as well as the offset of the profile was studied in detail. It has been concluded that the strike length has an insignificant role to play in the inversion as long as the profile bisects the fault plane. Inversion of gravity anomalies of the Aswaraopet master fault of the Chintalpudi sub-basin in India using the simulated parabolic density function yielded a geologically plausible model that is consistent with the borehole information.

1. Murthy, I. V. R., *Gravity and Magnetic Interpretation in Exploration Geophysics*, Memoir 40, Geological Society of India, Bangalore, 1998, p. 101.
2. Singh, B. and Guptasarma, D., New method for fast computation of gravity and magnetic anomalies from arbitrary polyhedra. *Geophysics*, 2001, **66**, 521–526.
3. Peirce, J. W. and Lipkov, L., Structural interpretation of the Rukwa Rift, Tanzania. *Geophysics*, 1988, **53**, 824–836.
4. Sclater, J. G. and Christie, P. A. F., Continental stretching: an explanation of the post mid-Cretaceous subsidence of the Central North Sea Basin. *J. Geophys. Res.*, 1980, **85**, 3711–3739.
5. Ferguson, J. F., Felch, R. N., Aiken, C. L. V., Oldow, J. S. and Dockery, H., Models of the Bouguer gravity and geologic structure at Yucca Flat, Nevada. *Geophysics*, 1988, **50**, 231–244.
6. Abdoh, A., Cowan, D. and Pilkington, M., 3D gravity inversion of the Cheshire basin. *Geophys. Prospect.*, 1990, **38**, 999–1011.
7. Hinze, W. J., Bouguer reduction density: why 2.67? *Geophysics*, 2003, **68**, 1559–1560.
8. Cordell, L., Gravity anomalies using an exponential density-depth function – San Jacinto Graben, California. *Geophysics*, 1973, **38**, 684–690.
9. Garcia-Abdeslem, J., Gravitational attraction of a rectangular prism with depth-dependent density. *Geophysics*, 1992, **57**, 470–473.
10. Chakravarthi, V., Gravity interpretation of non-outcropping sedimentary basins in which the density contrast decreases parabolically with depth. *Pure Appl. Geophys.*, 1995, **145**, 327–335.
11. Paul, M. K., Dutta, S. and Banerjee, B., Direct interpretation of two dimensional structural faults from gravity data. *Geophysics*, 1966, **31**, 940–948.
12. Sundararajan, N., Mohan, N. L. and Rao, S. V. S., Gravity interpretation of 2D fault structures using Hilbert transforms. *J. Geophys.*, 1983, **53**, 34–41.
13. Chakravarthi, V., Digitally implemented method for automatic optimization of gravity fields obtained from three-dimensional density interfaces using depth-dependent density. US Patent 6,615,139, 2003.
14. Chakravarthi, V. and Sundararajan, N., Ridge regression algorithm for gravity inversion of fault structures with variable density. *Geophysics*, 2004, **69**, 1394–1404.
15. Marquardt, D. W., An algorithm for least squares estimation of nonlinear parameters. *J. Soc. Ind. Appl. Math.*, 1963, **11**, 431–441.
16. Agarwal, B. P., Hydrocarbon prospects of the Pranhita–Godavari Graben, India. *Proc. Petrotech.*, 1995, **95**, 115–121.
17. Chakravarthi, V. and Sundararajan, N., Automatic 3-D gravity modeling of sedimentary basins with density contrast varying parabolically with depth. *Comput. Geosci.*, 2004, **30**, 601–607.

ACKNOWLEDGEMENTS. I thank the anonymous reviewers and the reviewing editor for their critical comments and suggestions to improve the manuscript. I also thank Dr V. P. Dimri, Director, National Geophysical Research Institute, Hyderabad for encouragement and permission to publish this paper, and Council of Scientific and Industrial Research, New Delhi for financial assistance under the Young Scientist project.

Received 25 February 2008; revised accepted 24 September 2008